



Article

Microwave-Assisted *Dendropanax morbifera* Extract for Cosmetic Applications

Hien Thi Hoang¹, Jae-Seok Park², Seong-Hyeon Kim¹, Ju-Young Moon^{3,*} and Young-Chul Lee^{1,4,*} 

¹ Department of BioNano Technology, Gachon University, Seongnam-Daero 1342, Sujeong-gu, Seongnam-si 13120, Korea; hienhoangh2t96@gmail.com (H.T.H.); shaera@gachon.ac.kr (S.-H.K.)

² Nature Fairy Co., Ltd., 3F, 28-27, Dongseo-ro 857 beon-gil, Siheung-si 14983, Korea; ournaturefairy@naver.com

³ Department of Beauty Design Management, Hansung University, 116 Samseongyoro-16gil, Seoul 02876, Korea

⁴ Well Scientific Laboratory Ltd., 305, 3F, Mega-center, SKnTechnopark, 124, Sagimakgol-ro, Jungwon-gu, Seongnam-si 13207, Korea

* Correspondence: bora7033@naver.com (J.-Y.M.); dreamdbs@gachon.ac.kr (Y.-C.L.)

Abstract: Recently, utilizing natural bioactive compounds for active ingredients in cosmetics has become a growing worldwide trend. More and more studies aim to identify the sources of herbal ingredients for applications in the pharmaceutical and cosmetic fields. Additionally, in order to optimize the safety of natural ingredients, choosing an environmentally friendly extraction method also plays an important role. In this work, an eco-friendly extraction technique for *Dendropanax morbifera* using microwave treatment and microwave-assisted *Dendropanax morbifera* extract (MA-DME) was investigated. The results indicate that higher yields of MA-DME were obtained than with conventional methods and that *D. morbifera*'s antioxidant properties were enhanced. Moreover, we found that MA-DME exhibited extraordinary antioxidant, anti-aging, and skin-whitening activities. We suggest MA-DME as a potential cosmeceutical ingredient than could be utilized for comprehensive protection of human skin.

Keywords: *Dendropanax morbifera*; microwave-assisted extraction; cosmetic applications; cosmeceutical ingredient; cytotoxicity



Citation: Hoang, H.T.; Park, J.-S.; Kim, S.-H.; Moon, J.-Y.; Lee, Y.-C. Microwave-Assisted *Dendropanax morbifera* Extract for Cosmetic Applications. *Antioxidants* **2022**, *11*, 998. <https://doi.org/10.3390/antiox11050998>

Academic Editors: Acácio Antonio F. Zielinski and Aline Alberti

Received: 25 April 2022

Accepted: 17 May 2022

Published: 19 May 2022

Publisher's Note: MDPI stays neutral with regard to jurisdictional claims in published maps and institutional affiliations.



Copyright: © 2022 by the authors. Licensee MDPI, Basel, Switzerland. This article is an open access article distributed under the terms and conditions of the Creative Commons Attribution (CC BY) license (<https://creativecommons.org/licenses/by/4.0/>).

1. Introduction

Not long ago, a global trend toward the use of natural bioactive substances as cosmetic agents took shape, due to their effective and biologically active substances and growing interest in skin care [1]. Currently, the global introduction of plant extracts is focused on applications with high added value, given that plant extracts contain bioactive ingredients including vitamins or minerals. Most of the components are of great interest to the preparation of natural products in cosmetics [2]. The bioactive components from plant extracts can be used as cosmeceutical formulations and achieve benefits including the maintenance of skin structure or function. In order to optimize the safety of natural ingredients, choosing an environmentally friendly extraction method also plays an important role. Microwave-assisted extraction (MAE) has been indicated as a promising technique for the extraction of medicinal plants for research as well as a green approach [3]. MAE provides effective extraction performance with less or no solvent consumption, as well as protection with rapid and high extraction yields for thermolabile constituents. MAE showed advantages that are more effective and cheaper than conventional extraction methods such as Soxhlet, percolation, extraction under reflux, and sonication [4]. In addition, MAE allowed higher recoveries without altering the antioxidant potential of the extracts [5]. Hence, MAE is one of the most suitable solutions for green and natural products.

Dendropanax morbifera (*D. morbifera*), a native plant of South Korea, is known as a medicinal herb used for the comprehensive treatment of human illnesses [6] such as

hyperglycemia, hair loss, and skin disorders [7–9]. It is reported that many bioactive compounds were included in *Dendropanax* plant species [10]. Many scientific reports have previously highlighted that the main bioactive compounds of *D. moribifera* are quercetin, chlorogenic acid, rutin, carnosol, dextromethorphan, cannabidiol, bremazocine, doxapram, etc. [11,12]. Furthermore, previous studies reported that *D. moribifera* exhibits antioxidant [13,14], anti-inflammatory [15,16], neuroprotective [6,17], osteosarcoma [18], anti-diabetic [19,20], hepatoprotective [21,22], immunomodulatory [16,23], antibacterial and antifungal [24], antiplasmodial [25], cytotoxic [26], and larvicidal [27] functions. Recently, interest in *D. moribifera* as a functional material in cosmetics has increased thanks to its well-rounded health benefits for humans. There are several reports that *D. moribifera* and its components shows anti-wrinkle, hair growth, and moisturizing effects [7,28]. Especially, β -sitosterol, isolated from *D. moribifera*, provides skin whitening and moisturizing effects, prevention of hair loss, and hair density improvement [28]. Moreover, *D. moribifera* leaf extract considerably reduces melanin content, suggesting it as a candidate for a skin-whitening agent [29].

In the present study, we focused on extracting the bioactive compounds in *D. moribifera* by the microwave-assisted method. To further investigate the efficacy of MAE, the active ingredients in microwave-assisted *D. moribifera* extract (MA-DME) were identified by ultra-high performance liquid chromatography with mass spectrometry (UHPLC-MS). In addition, we evaluated the antioxidant, anti-wrinkle, whitening and moisturizing effects to investigate the potential of *D. moribifera* extract as a promising ingredient for cosmetic formulations.

2. Materials and Methods

2.1. Materials

D. moribifera was grown and harvested in Wando, Korea. Methanol and acetonitrile were purchased from Honeywell Burdic & Jackson (Morristown, NJ, USA). Formic acid, sodium carbonate (Na_2CO_3), and aluminum chloride hexahydrate ($\text{AlCl}_3 \cdot 6\text{H}_2\text{O}$) were purchased from Daejung Chemicals & Metals Co., Ltd. (Siheung-si, Korea). EZ-cytox solution was purchased from DoGenBio (Guro-gu, Korea). Tris-HCl buffer, PBS, and Tris solution buffer were purchased from Thermo Fisher Scientific (Waltham, MA, USA). Folin–Denis reagent, kojic acid, elastase, mushroom tyrosinase, 2,2'-azino-bis(3-ethylbenzothiazoline-6-sulfonic acid) (ABTS), Cell Proliferation Kit I (MTT), DMSO, L-ascorbic acid, gallic acid, and quercetin were purchased from Sigma Aldrich (St. Louis, MO, USA)

2.2. Microwave-Assisted *Dendropanax moribifera* Extract (MA-DME)

For the preparation of raw *D. moribifera*, dry leaves and wood of *D. moribifera* were thoroughly soaked in water, then sliced into small pieces. Next, 20 g of the sliced raw materials were ground into a homogenous mixture using a blender. *D. moribifera* powder was obtained by utilizing a freeze-dryer and diluting in various concentrations with DI water. DI water was obtained utilizing Milli-Q Millipore filter system (Millipore Co., Billerica, MA, USA) with conductivity of $<18.2 \text{ M}\Omega \cdot \text{cm}^2$.

A microwave oven (Magic MMO-20M7, SK magic, Jongno-gu, Korea) was utilized in this work. The extraction of MA-DME was carried out referring to the method of Alvand et al. (Figure 1) [30,31]. Raw *D. moribifera* was irradiated for 10 min under microwave (800 W). The irradiated *D. moribifera* was cooled in ambient temperature and ground into powder. Once the sample was cooled, 20 mL of DI water was added and filtered through 0.22 μm filter. The MA-DME was freeze-dried to obtain extract powder.

The extraction yield Y (%) of MA-DME was expressed in the following equation:

$$Y(\%) = \frac{W_1}{W_2} \times 100$$

where W_1 is the weight (g) of pure MA-DME powder, while W_2 is the weight (g) of the initial *D. moribifera* powder. Calculated extraction yield was about 33.5%.

To compare the extraction efficiency of MAE with conventional extraction, we prepared Black extract 5% and Transparent extract 5% as control samples. Therein, Black extract 5% was a non-carbonized black extract of *D. morbifera*. After obtaining the pulverized *D. morbifera* particles as in MA-DME, the Black extract was obtained by bathing in water at 100 °C. Additionally, Transparent extract 5% was a non-carbonized transparent extract of *D. morbifera*. After obtaining the pulverized *D. morbifera* particles as in MA-DME, it was subjected to distillation extraction using DI water at 100 °C to obtain a liquid extract through a cooling machine.

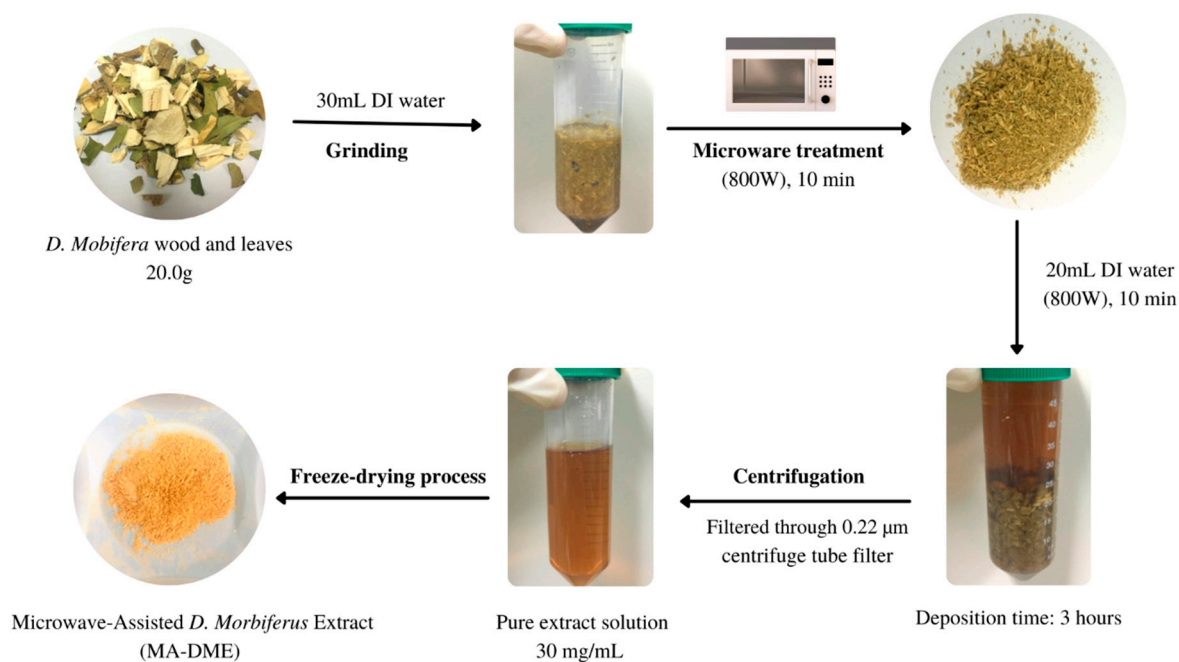


Figure 1. The extraction process for MA-DME.

2.3. Ingredient Analysis of MA-DME

The active compounds of *D. morbifera* were characterized by an ultra-high performance liquid chromatography system loaded with a mass spectrometer (UHPLC-MS) equipped with an electrospray ionization source (ESI). The HPLC separation was conducted on an ACQUITY UPLC HSS T3 column (1.8 µm) with the following parameters: runtime: 25 min; solvent A: formic acid; solvent B: acetonitrile; flow rate: 0.5 mL/min; gradient program: 0 min: 97% A, 0–1 min: 97% A, 1–15 min: 100% B, 15–16 min: 100% B, 16–19 min: 97% A, 19–25 min: 97% A; wavelength: 265 nm; column temperature: 35 °C; sample temperature: 12 °C; injection volume: 5 µL. The mass spectrometer was operated with the following parameters: capillary voltage: 3.0 kV (positive) and 2.8 kV (negative); resolution: 20,000; mass range scanned: 50–1200 m/z; nebulizer pressure: 6.4 Bar; drying gas temperature: 500 °C; drying gas flow rate: 800 L/h.

2.4. Antioxidant Content Analysis of MA-DME

Folin–Denis reagent was utilized for measurement of total polyphenol content [32]. A 100 µL amount of MA-DME and 900 µL of DI water were mixed into a conical tube. Then, 100 µL of Folin–Denis reagent were added and incubated at room temperature for 3 min. A 200 µL amount of 10% Na₂CO₃ was added after reaction, and the solution was topped up to 2 mL with DI water. The solution was allowed to react for 1 h in the darkroom, and absorbance of the solution was measured at 760 nm using a UV-Vis spectrophotometer (Varian Cary 50 UV-vis spectrophotometer, Agilent Technologies Inc., Santa Clara, CA, USA). The standard calibration curve of gallic acid (GA) was used for calculating total polyphenol content.

Total flavonoid content was also evaluated using modified methods of Woisky and Salatino [33]. In this study, methanolic solutions of quercetin with various concentrations (5–50 µg/mL) were used as references. A 0.6 mL amount of reference solution and 50 mg/mL of MA-DME extract were mixed with 0.6 mL of 2% AlCl₃. Mixed solutions were incubated at room temperature for 1 h. After incubation, measurement of absorbance was carried out with a UV-Vis spectrophotometer at 420 nm. Determination of total flavonoid content was conducted with quercetin standard curve.

2.5. Cell Viability Assay

The effects of MA-DME, Black extract, and Transparent extract on cell viability were evaluated with an MTT assay in 96-well plates. HaCaT cells were seeded at a density of 1·10⁵ cells and incubated in 37 °C, 5% CO₂ conditions for 24 h. After that, various concentration of MA-DME (0 to 300 µg/mL) were treated and incubated for 24 h or 48 h. Then, 10 µL of EZ-cytox solution was added to each well, and the well plate was incubated for 4 h. Finally, measurement of absorbance at 450 nm wavelength was carried out utilizing a plate reader (Multi-label plate reader, PerkinElmer, Boston, MA, USA).

2.6. Evaluation of Intracellular Reactive Oxygen Species (ROS)

Dichloro-dihydro-fluorescein diacetate (DCFH-DA) assay was performed to measure the generation of intracellular reactive oxygen species. HaCaT (2.5·10⁵ cells/mL) seeded black 96-well plates (Thermo Fisher Scientific, Waltham, MA, USA) were treated with test compounds at a concentration of 0–300 µg/mL and incubated for 24 and 48 h. Then, 10 µM DCFH-DA, which were diluted in DMSO, were allowed to stain for 1 h in a darkroom and washed twice with PBS buffer. In the literature, DCFH-DA penetrates into the internal cells and is then hydrolyzed into DCFH by esters; it was recorded by fluorescence measurement at 485/530 nm immediately. Dipyrindamole was used as a control with the relative ROS level of 100%. Generation of ROS was expressed with the following formula:

$$ROS\ Generation(\%) = \frac{F}{F_0} \times 100$$

where F is the fluorescence intensity of cells pretreated with MA-DME; F_0 is the fluorescence intensity of dipyrindamole.

2.7. ABTS Radical Preparation Protocol

The antioxidant capacities were measured by ABTS assay using a recent method with a slight modification [34]. The Black extract and MA-DME were suspended in dimethyl sulfoxide (DMSO), and the DMSO alone was used as a negative control. L-Ascorbic acid (Vitamin C) and quercetin were used as antioxidant standards and diluted with DMSO at 10 mg/mL. After 50 µL/well of test compounds were added in the 96-well plate, 150 µL of the ABTS radical was added into each well. Then, absorbance was read at 734 nm at room temperature for 5, 15, and 30 min of incubation time, and initial absorbance was 0.7 (CLARIOstar Microplate Reader, BMG Labtech Inc., Cary, NC, USA). Radical scavenging activity of test compounds was expressed as inhibition of absorbance (I_a , %) using the following formula:

$$I_a(\%) = 100 - \left[\frac{\mu\text{Extract absorbance}}{\mu\text{DMSO absorbance}} \times 100 \right]$$

where $\mu\text{Extract absorbance}$ is the absorbance of test compounds, μDMSO is the absorbance of the DMSO.

2.8. Tyrosinase Inhibitory Activity Assay

The tyrosinase inhibitory activity was measured with reference to a previously reported method [35]. L-DOPA was used as substrate in this assay. A 40 µL amount of 10 mM

L-DOPA was mixed with 80 μL of phosphate buffer (0.1 M, pH 6.8) in a 96-well plate and incubated for 10 min at 37 $^{\circ}\text{C}$. A 40 μL amount of MA-DME or Black or Transparent extract (50, 100, 200, 400, 800, and 1000 $\mu\text{g}/\text{mL}$) and 40 μL of mushroom tyrosinase (250 U/mL, in PBS) were then added to each well. Absorbance of the mixtures was read at 475 nm utilizing a microplate reader (Multi-label plate reader, PerkinElmer, Boston, MA, USA) at 1 min intervals over a period of 120 min. PBS was used as a blank control and Kojic acid (50 $\mu\text{g}/\text{mL}$) and L-ascorbic acid (50 $\mu\text{g}/\text{mL}$) were used as positive controls. The inhibition for each enzyme assay was expressed as follows:

$$\text{Inhibition}(\%) = \left[\frac{\text{control OD} - \text{Sample OD}}{\text{Control OD}} \right] \times 100$$

where Control OD indicates the difference in absorbance of control between incubation times, and Sample OD indicates the difference in absorbance of sample between incubation times.

Each experiment was performed in triplicate ($n = 3$), and the IC_{50} value was calculated from the dose–response curves by nonlinear regression analysis using GraphPad Prism software version 5.0 (GraphPad software Inc., San Diego, CA, USA).

2.9. Elastase Inhibitory Effect Assay

Assessment of elastase inhibition was conducted by the intensity of the solution color assay referring to the method of Tu and Tawata [36]. N-Succinyl-Ala-Ala-Ala- ρ -nitroanilide (AAAVN) elastase substrate was diluted with 0.1232 M Tris-HCl buffer solution (pH 8) to make a 1.0 mM concentration. Then, the elastase substrate was mixed with the 10 μL of sample in the 96-well plates and pre-incubated at 25 $^{\circ}\text{C}$ for 10 min. After pre-incubation, the reaction was initiated by adding 10 μL of elastase from porcine pancreas (7.5 units/mL) in Tris solution buffer to the pre-incubated mixtures. Finally, a microplate reader (Multi-label plate reader, PerkinElmer, Boston, MA, USA) was utilized to measure the absorbance at 410 nm.

2.10. Blue Light Penetration Experiment with MA-DME

MA-DME was prepared by dilution at concentrations of 3.75, 7.5, 15, and 30 mg/mL. The 400–450 nm wavelength band of blue light was tested for blocking or transmission with DI water, as control sample, by using a black night UV lamp (ROBUST UV 12LED, Campnic, Uijeongbu-si, Korea).

3. Results and Discussion

3.1. Characterization of MA-DME

The UHPLC-MS chromatogram identified 33 major compounds in *D. morbifera* extract (Figure 2, Table 1). As listed in Table 1, we found that *D. morbifera* extract contains many phenolic and flavonoid compounds known as natural antioxidants, such as 1-*O*-Caffeoylquinic acid, 4-*O*-Caffeoylquinic acid, and Corchoionoside, 3,7,8,3',4'-Pentahydroxyflavone, whereas apocynoside I inhibits CYP2C9, which causes aging and lowers disease resistance, and Viscumneoside III inhibits tyrosinase, which impedes skin whitening [37].

Quercetin is known to inhibit MMP-1, which encourages the imbalance or collapse of collagen molecules in UV-irradiated skin [38].

Table 1. Identified compounds in MA-DME.

No	Compound	Formula	Ion Mode	Retention Time	Extract Mass (m/z)	Suggested Role
1	Quinic acid	C ₇ H ₁₂ O ₆	–	0.59	191.0558	Astringent, anti-viral
2	1-O-Caffeoylquinic acid	C₁₆H₁₈O₉	–	2.95	353.0874	Phenolic acid, antioxidant, antibacterial, anticancer, antihistamine, anti-viral
3	4-O-Caffeoylquinic acid	C ₁₆ H ₁₈ O ₉	–	3.52	353.0871	
4	3-[(4-O-Acetyl-6-deoxy-α-L-mannopyranosyl)-oxyl]-2-(3,4-dihydroxyphenyl)-5-hydroxy-6-methoxy-4-oxo-4H-chromen-7-yl 2-O-acetyl-6-deoxy-α-L-mannopyranoside	C₃₂H₃₆O₁₈	–	3.43	707.1825	Flavonoids
5	Benzyl alcohol xylopyranosyl(1->6)glucopyranoside	C ₁₈ H ₂₆ O ₁₀	–	3.71	401.1437	Tea aroma glycosidic precursor bioactivation
6	Apigenin-6-C-glucosylglucoside (Isovitexin)	C₂₇H₃₀O₁₅	– +	3.79 3.79	593.1497 595.2663	Anti-inflammatory, antioxidant, antibacterial, anti-Alzheimer's disease, anti-diabetic, anti-viral
7	Apocynoside I	C₁₉H₃₀O₈	–	3.86	431.1901	Inhibition of CYP2C9—causing aging and lowered disease resistance
8	Corchoionoside C	C₁₉H₃₀O₈	–	3.86	431.1909	Flavonoids
9	1,3-Dihydroxy-2-hydromethylanthraquinone-3-B- β -D-xylopyranose(1->6)- β -D-glucopyranoside	C ₁₆ H ₂₈ O ₁₄	– +	4 3.99	563.1395 565.2557	N/A
10	Apiin	C ₁₆ H ₂₈ O ₁₄	– +	4.09 4.09	563.1402 565.1562	Anxiolytic, anti-inflammatory , anti-cancer, anti-fungal
11	Isochaftoside	C ₁₆ H ₂₈ O ₁₄	–	4.23	563.1399	Flavones
12	7-O-β-D-glucopyranosylkaempferol	C₂₁H₂₀O₁₁	– +	4.24 4.13	447.0924 449.1083	Anti-inflammatory, anti-cancer, anti-diabetes <i>Inhibit vascular endothelial inflammation</i> <i>Protect the cranial nerve and heart function</i> <i>Treat fibroproliferative disorders, anti-viral</i>
13	Kaempferol-3,7-di-O-β-D-glucopyranoside	C₂₇H₃₀O₁₆	– +	4.46 4.46	609.1453 611.1618	
14	Nelumboside A	C ₂₇ H ₃₀ O ₁₆	–	4.57	609.1450	Antioxidant
15	3,8-Di-C-glucosylapigenin	C ₂₇ H ₃₀ O ₁₅	–	4.79	593.1499	N/A
16	Genistein-7,4'-di-O-β-D-glucoside	C₂₇H₃₀O₁₅	–	4.79	593.1499	<i>Prevents hypertension, anti-cancer, maintaining bone mineral density, anti-Alzheimer's disease, anti-viral</i>

Table 1. Cont.

No	Compound	Formula	Ion Mode	Retention Time	Extract Mass (m/z)	Suggested Role
17	Terestigmine	C ₂₁ H ₃₃ N ₃ O ₃	–	9.08	374.2436	Cholinesterase inhibitor (treatment of cognition disorders)
18	N-(3-Methoxy-5-nitrophenyl)-2-(5-methyl-3,4-dinitro-1H-pyrazol-1-yl)acetamide	C ₁₃ H ₁₂ N ₆ O ₈	+	0.56	381.0795	N/A
19	Guanine	C ₅ H ₅ N ₅ O	+	1.45	152.0566	Nucleobases
20	Daidzein-4',7-diglucoside	C ₂₇ H ₃₀ O ₁₄	+	4.42	579.1728	Phytoestrogen
21	Viscidulin I	C ₁₅ H ₁₀ O ₇	+	4.46	303.0502	Inhibitor of hepatocellular carcinoma cells (protein Glypican-3)
22	Viscumneoside III	C ₂₅ H ₂₆ O ₁₃	+	4.47	535.1454	Tyrosinase inhibition (skin whitening)
23	<i>Aloe emodin 8-glucoside</i>	C ₂₁ H ₂₀ O ₁₀	– +	4.51 4.51	431.0971 433.1132	<i>Anti-diabetic, DNA targeting molecule, anti-viral</i>
24	3,7,8,3',4'-Pentahydroxyflavone (Quercetin)	C₁₅H₁₀O₇	+	4.63	303.0499	Strong antioxidant flavonoids, xanthine oxidase inhibition, antihyperuricemic, anti-inflammatory, enhances immune-regulation
25	Rubianic acid (dithiooxamide)	C ₂₅ H ₂₆ O ₁₃	+	4.65	535.1451	Chelating agent (detection of copper), building block in the synthesis of cyclen
26	<i>3-Hydroxy baicalein</i>	C₁₅H₁₀O₆	+	4.79	287.0548	<i>Anxiolytic, antiestrogen, anti-inflammatory, anti-cancer, antibacterial, anti-viral</i>
27	7-Hydroxy-1-methoxy-2-methoxyxanthone	C ₁₅ H ₁₀ O ₆	+	4.79	287.0548	N/A
28	6,6'-Iminobis(2,2-dimethyl-1-hexanol)	C ₁₆ H ₃₅ NO ₂	+	7.7	274.2738	N/A
29	N~2~-(2S,4S,5S)-5-Amino-6-cyclohexyl-4-hydroxy-2-isopropylhexanoyl]-N-[2-pyridinylmethyl]-L-isoleucinamide	C ₂₇ H ₄₆ N ₄ O ₃	+	9.08	475.3646	N/A
30	4-N-([1,2,4]triazolo[4,3-a]pyridin-3-ylmethyl)butanamide	C ₁₉ H ₂₇ N ₉ O	+	9.08	398.2415	N/A
31	1-Methyl-2-[(Z)-8-tetradecenyl]-4(1H)-quinolone	C ₂₄ H ₃₅ NO	+	9.08	276.2596	N/A
32	O-Benzyl-N-[9-(1H-imidazol-1-yl)nonanoyl]-L-seryl-N~6~-(benzyloxy)carbonyl]-N-(2-cyclohexylethyl)-L-lysineamide	C ₄₄ H ₆₄ N ₆ O ₆	+	9.08	773.4956	N/A

Bold: Main phenolic and flavonoid compounds. Italic and Bold: Potential cosmetic compounds.

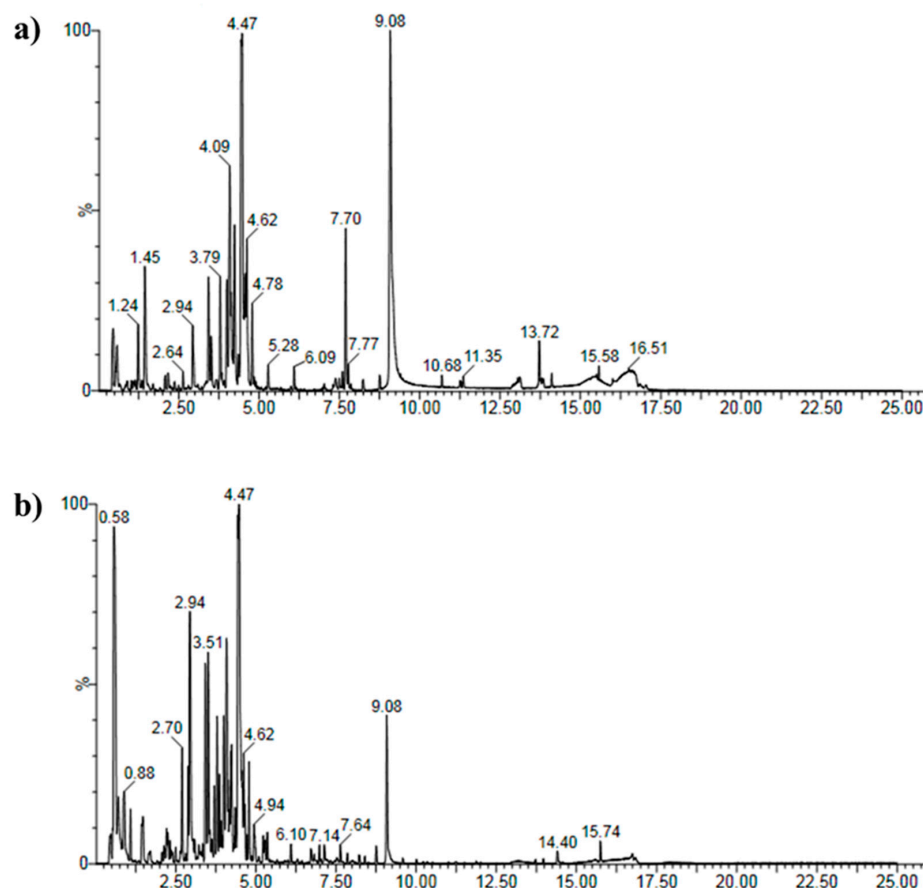


Figure 2. High-resolution extracted ion chromatograms for MA-DME: (a) positive ion mode; (b) negative ion mode.

3.2. Total Contents of Phenols and Flavonoids

Total amounts of phenols were evaluated by modified Folin–Ciocalteu method and expressed as gallic acid equivalents per μg dry weight of plant extract ($\text{GAE } \mu\text{g}^{-1} \text{ DW}$). A calibration curve for quantification of phenolic compounds in samples was prepared using gallic acid at a concentration of 50 to 500 $\mu\text{g}/\text{mL}$. The calibration curve was formed as a graph of $y = 0.02992 + 0.00112x$ ($R^2 = 0.9969$) (Figure S1). The absorbance measurement results are shown in Figure S2 and Table S1. From the above results, it was found that the phenolic compounds were contained in an amount of 313.03 $\text{GAE } \mu\text{g}^{-1} \text{ DW}$ in MA-DME, 252.25 $\text{GAE } \mu\text{g}^{-1} \text{ DW}$ in Black extract 5%, and 30.57 $\text{GAE } \mu\text{g}^{-1} \text{ DW}$ in Transparent extract 5% (Table 2).

Table 2. Total phenolic content and flavonoid content in MA-DME.

Sample	Total Phenols (mg GAE g^{-1})	Total Flavonoids (mg QE g^{-1})
MA-DME	313.03 ± 3.9	32.37 ± 0.9
Black extract 5%	252.25 ± 6.9	21.04 ± 1.1
Transparent extract 5%	30.59 ± 4.2	0

In addition, the concentrations of total flavonoids in *D. morbifera* were determined by the modified Woisky and Salatino method and expressed in quercetin equivalents per μg dry weight of plant extract ($\text{QE } \mu\text{g}^{-1} \text{ DW}$). The calibration curve was formed as a graph of $y = 0.005 + 0.0298x$ ($R^2 = 0.9841$) (Figure S3). The absorbance measurement results are shown in Figure S4 and Table S2. From the above results, it was found that flavonoids were

contained in an amount of $32.37 \text{ QE } \mu\text{g}^{-1} \text{ DW}$ in MA-DME, $21.04 \text{ QE } \mu\text{g}^{-1} \text{ DW}$ in Black extract 5%, and $0 \text{ QE } \mu\text{g}^{-1} \text{ DW}$ in Transparent extract 5% (Table 2).

In general, the extract of MA-DME was found to have very high contents of both phenolics and flavonoids, compared to the contents in Black and Transparent extracts. It could be explained that microwave treatment heats the material toward its volume while the conventional heating process heats from the outside of the material and requires contact with a hot outer surface. Thus, internal change within a short time leads to pressure increase inside the plant cells, which further breaks the cell walls and releases the desired molecules.

3.3. Cell Viability Assay

MA-DME did not reduce HaCaT cell viability in concentrations of up to $100 \mu\text{g}/\text{mL}$, both after 24 h and 48 h, but slightly decreased viability at $200 \mu\text{g}/\text{mL}$ after 48 h (Figure 3). These results determined the survival of human keratinocyte HaCaT cells with treatment of MA-DME in various concentrations (10 to $300 \mu\text{g}/\text{mL}$). Transparent extract was non-toxic to HaCaT cells at low concentrations ($\leq 200 \mu\text{g}/\text{mL}$) and caused negligible toxicity at higher concentrations ($300 \mu\text{g}/\text{mL}$).

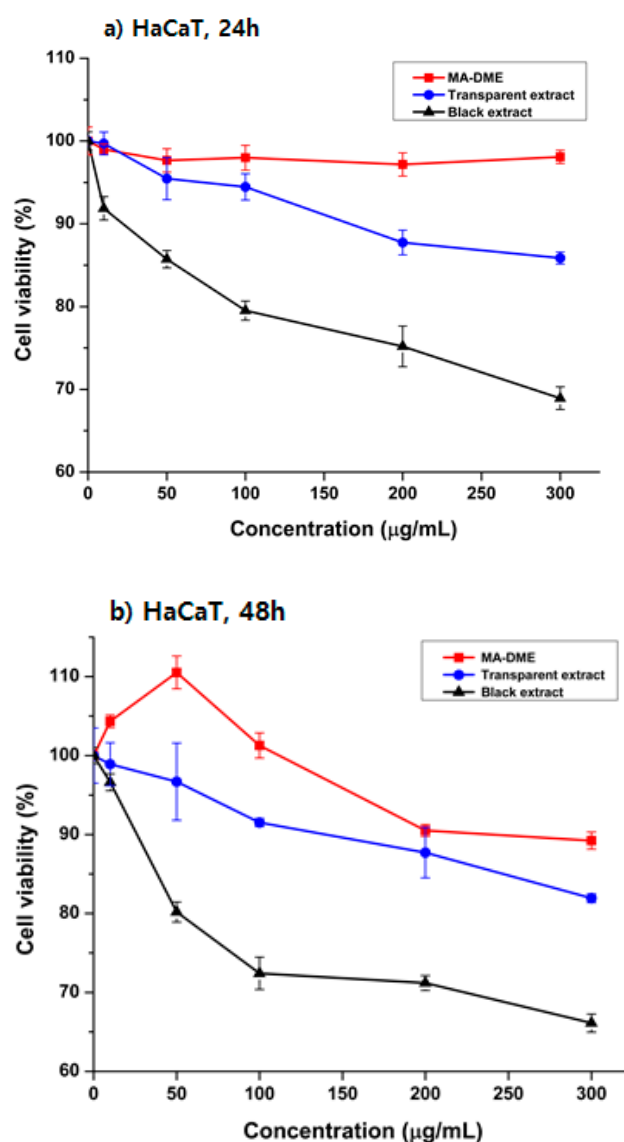


Figure 3. The effect of MA-DME on the viability of HaCaT cells compared with Black extract and Transparent extract for (a) 24 h, (b) 48 h. The viability of MA-DME (10 to $300 \mu\text{g}/\text{mL}$) was measured via MTT assay, $n = 3$.

3.4. MA-DME Effect on Reactive Oxygen Species (ROS)

The ROS measurements demonstrated that the Transparent extract does not produce ROS radicals in either short or long-term treatment, which may explain that this extract contained a large amount of anti-oxidant compounds. Although the Black extract showed slightly higher toxicity than the Transparent extract and MA-DME, it could be considered to be less toxic to HaCaT cells because more than 60% of the cells could survive at its high concentration (300 g/mL) (Figure 4). Furthermore, this extract also produced a small amount of ROS radicals, resulting in increases in relative DCF-fluorescence to control. In summary, MA-DME, rather than the Black extract and Transparent extract, could be possibly applied to cosmetics.

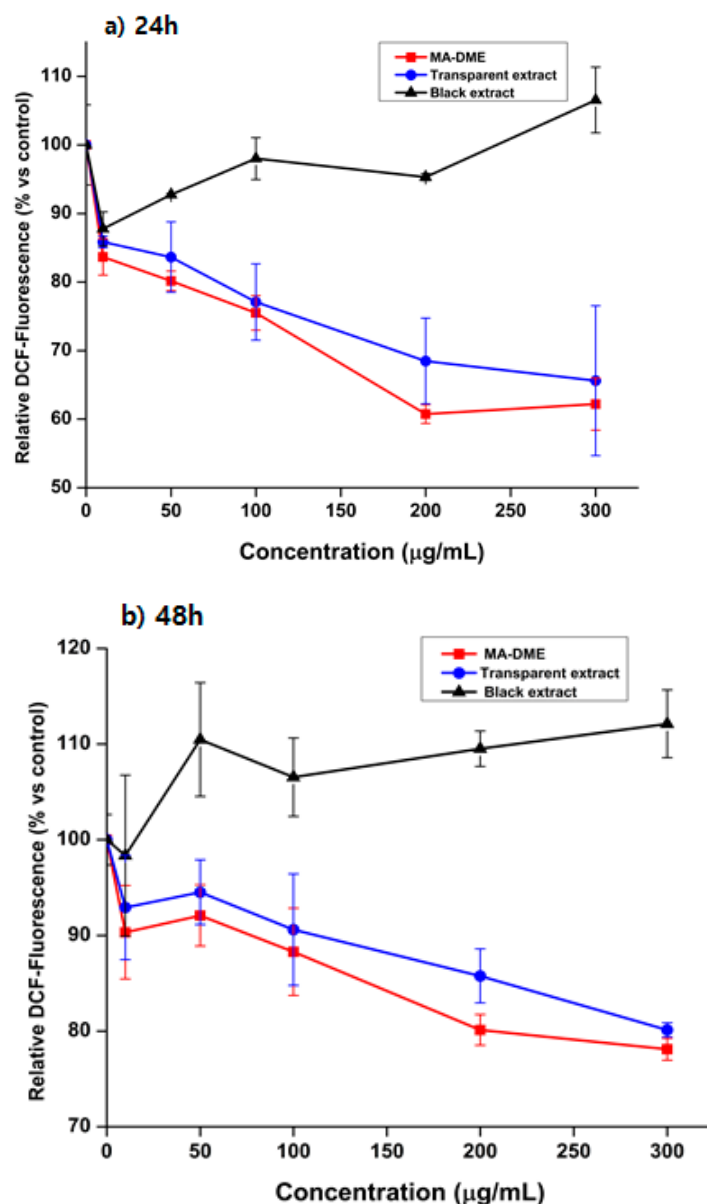


Figure 4. The effect of MA-DME on ROS compared with Black extract and Transparent extract for (a) 24 h, (b) 48 h, $n = 3$.

3.5. ABTS Free Radical Scavenging Activity

The radical scavenging activities of MA-DME and Transparent extracts were determined by their ABTS radical scavenging efficiency compared to L-ascorbic acid and quercetin (Figure 5). Radical scavenging activities of the MA-DME and Transparent extracts

showed concentration-dependent relationships. MA-DME exhibited slightly lower ABTS radical scavenging activities than L-ascorbic acid and quercetin did. On the other hand, the radical scavenging activities of the Transparent extracts were very low, compared with MA-DME, and Transparent extracts only showed a slight concentration-dependent increase in activity.

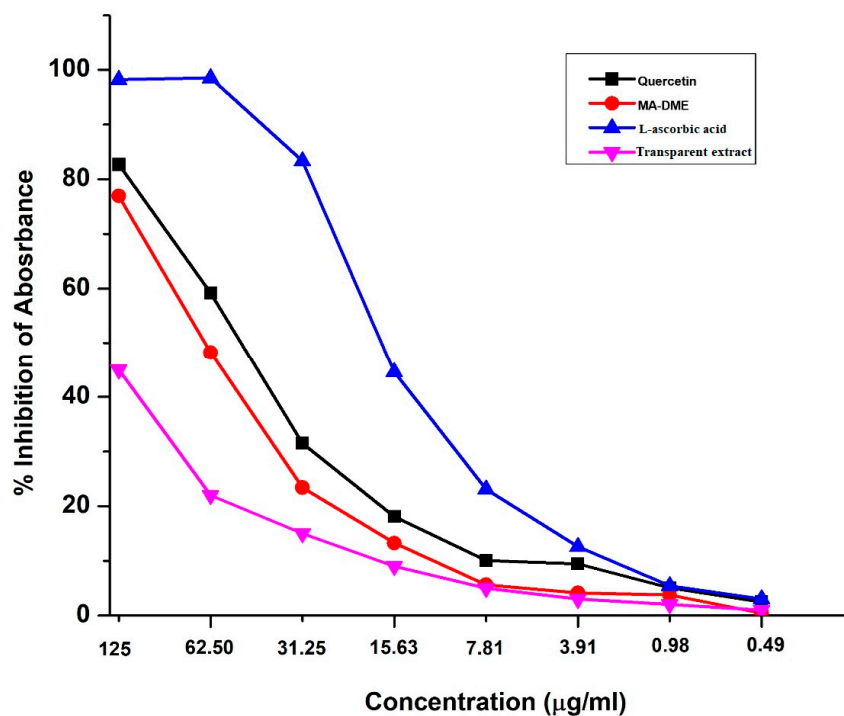


Figure 5. ABTS radical scavenging activity of MA-DME and Transparent extract.

Extracellular matrix (ECM), the outermost skin part, consists of fibroblasts and protein including collagen and elastin [39]. Collagen and elastin are essential for maintaining skin richness and elasticity to keep it youthful and healthy [40,41]. Deposited ROS due to exposure to photo-aging factors can indirectly activate dermal enzymes such as collagenase and elastase, which basically break down and degrade collagen as well as elastin, respectively [42]. Additionally, external oxidative attacking factors influence the skin and have to cope with the endogenous generation of ROS and other free radicals, which are produced continuously during cellular metabolism. Therefore, MA-DME with its high radical scavenging activities and ROS inhibition can be useful to prevent skin aging.

3.6. Tyrosinase Inhibitory Activity Assay

Deposits of melanin in the epidermal layer can cause undesired melanogenesis or skin pigmentation [43]. Melanogenesis could be regulated by inhibiting the activity of tyrosinase or other related enzymes. Tyrosinase, one of the melanogenic enzymes, is the rate-limiting enzyme that controls the production of melanin [44]. Thus, utilizing tyrosinase inhibitors is clearly a promising way to inhibit melanogenesis.

The potential of MA-DME to inhibit mushroom tyrosinase at concentrations from 50 to 1000 µg/mL was higher than that of Transparent extract (Figure 6). At concentrations of 50 and 100 µg/mL, MA-DME showed better tyrosinase inhibition effects than kojic acid, which is known as a whitening agent. Consequently, MA-DME is a promising whitening ingredient for cosmetics applications.

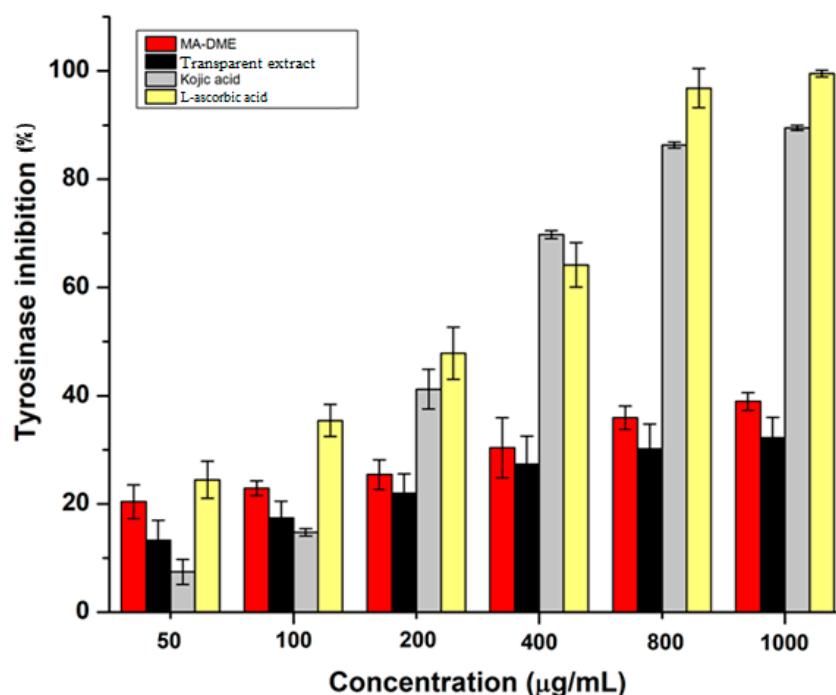


Figure 6. Tyrosinase inhibitory effects of MA-DME, Transparent extract and positive controls, $n = 3$.

3.7. Elastase Inhibitory Assay

Elastase is particularly responsible for the disruption of elastin, and elastin is a crucial protein present in the ECM. Elastin, due to its unique elastic recoil properties, is a crucial protein for imbuing elasticity to the skin [45,46]. With regard to anti-aging, seeking to inhibit elastase enzymes is valuable to avoid skin aging and the loss of skin elasticity.

To examine the effects of MA-DME on elastase effects, we determined the porcine elastase activity upon treatment with various concentrations of sample extract (Table 3).

Table 3. Inhibition activity (%) of MA-DME targeting porcine pancreas elastase activity (0.4 U/mL).

Concentration (µg/mL)	Elastase Inhibition Ratio (%) *		
	MA-DME	Retinol	Adenosine
6.25	4.6 ± 2.0	4.6 ± 2.5	3.5 ± 1.4
12.5	6.8 ± 2.4	13.8 ± 1.0	12.2 ± 0.88
25	13.1 ± 1.2	9.04 ± 3.0	11.8 ± 2.9
50	14.9 ± 1.7	13.6 ± 0.90	14.1 ± 1.0
100	14.1 ± 0.60	13.3 ± 0.21	8.7 ± 1.3
200	15.8 ± 0.61	11.0 ± 1.3	13.0 ± 1.5
400	16.0 ± 0.43	14.5 ± 0.70	13.7 ± 1.6

(Mean ± SD) MA-DME showed high elastase inhibition activity in a specific concentration range. Additionally, MA-DME at high concentrations (100 to 400 µg/mL) showed enhanced active elastase inhibition activity compared to the effect of retinol and adenosine. Therefore, MA-DME might have a potential role in improving skin elasticity and reducing wrinkles in skin.

$$* \text{ Elastase Inhibition Ratio}(\%) = 1 - \frac{\text{Absorbance of sample}}{\text{Absorbance of control}} \times 100$$

3.8. Blue Light Penetration Experiment with MA-DME

The experimental results are shown in Figure 7. MA-DME did not transmit blue light at concentrations of 30 mg/mL, 15 mg/mL, and 7.5 mg/mL. It was found that the blue

light was faintly transmitted in a sample at 3.75 mg/mL concentration. As such, MA-DME was shown to have a shielding ability against blue light. Therefore, MA-DME may have a skin-protecting effect against blue light.

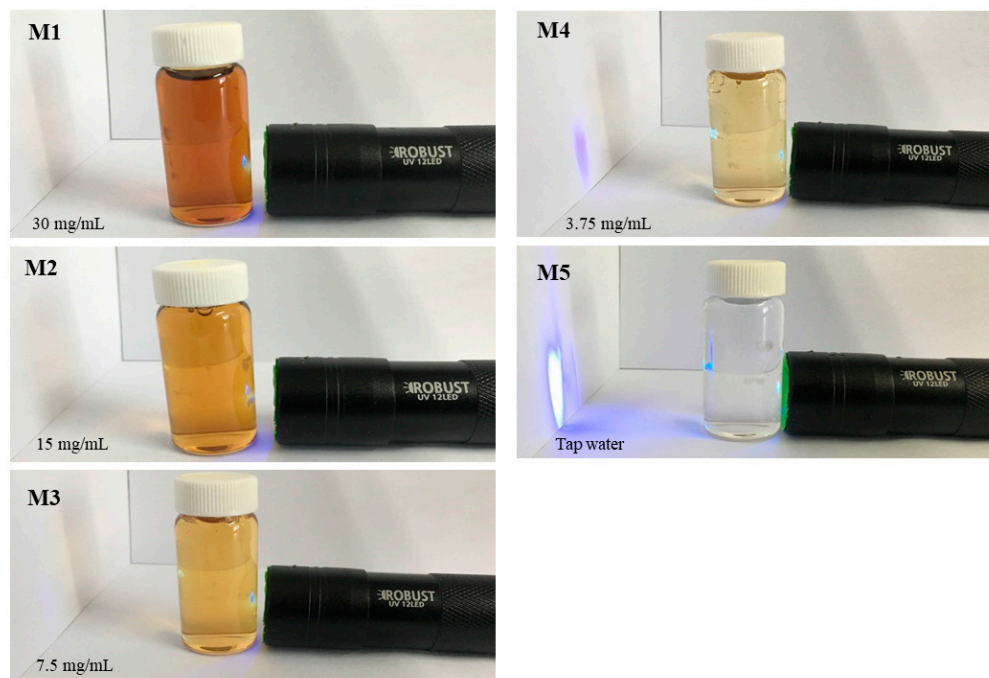


Figure 7. Results for blue light protection effects of MA-DME.

4. Conclusions

The results of this study showed that the microwave-assisted extraction method improved the bioactivities of *D. morbifera* in the resultant MA-DME. It was also found that MA-DME showed high biocompatibility, excellent antioxidant activity and whitening effects. Compared with Transparent extract or Black extract, the superior features of MA-DME including cell viability, total bioactive compound contents, radical scavenging effects, and tyrosinase inhibitory effects were shown in this work. Therefore, we suggest MA-DME as a promising candidate for cosmetic applications.

Supplementary Materials: The following supporting information can be downloaded at: <https://www.mdpi.com/article/10.3390/antiox11050998/s1>, Table S1. List of samples and the absorbance measurement results for evaluating phenolic; Table S2. List of samples and the absorbance measurement results for evaluating flavonoid; Figure S1. The calibration curve for quantification of phenolic compounds; Figure S2. The absorbance measurement results to evaluate the phenolic compounds; Figure S3. The calibration curve for quantification of flavonoid compounds; Figure S4. The absorbance measurement results to evaluate the flavonoid compounds.

Author Contributions: Conceptualization, H.T.H., J.-S.P., J.-Y.M., Y.-C.L.; data curation, H.T.H., S.-H.K.; writing original draft preparation, Kim, S.-H.K.; writing review and editing, S.-H.K.; funding acquisition, J.-S.P. All authors have read and agreed to the published version of the manuscript.

Funding: This work was supported by the Basic Science Research Program through the National Research Foundation of Korea funded by the Ministry of Education (2021R1F1A1047906) and by the Gachon University research fund of 2021 (GCU-202103310001).

Institutional Review Board Statement: Not applicable.

Informed Consent Statement: Not applicable.

Data Availability Statement: Data is contained within the article and supplementary material.

Conflicts of Interest: The authors declare no conflict of interest.

References

1. Amberg, N.; Fogarassy, C. Green Consumer Behavior in the Cosmetics Market. *Resources* **2019**, *8*, 137. [[CrossRef](#)]
2. Atanasov, A.G.; Waltenberger, B.; Pferschy-Wenzig, E.-M.; Linder, T.; Wawrosch, C.; Uhrin, P.; Temml, V.; Wang, L.; Schwaiger, S.; Heiss, E.H.; et al. Discovery and Resupply of Pharmacologically Active Plant-Derived Natural Products: A Review. *Biotechnol. Adv.* **2015**, *33*, 1582–1614. [[CrossRef](#)]
3. Mandal, V.; Mohan, Y.; Hemalatha, S. Microwave Assisted Extraction—An Innovative and Promising Extraction Tool for Medicinal Plant Research. *Pharmacogn. Rev.* **2007**, *1*, 7–18.
4. Vinatoru, M.; Mason, T.J.; Calinescu, I. Ultrasonically Assisted Extraction (UAE) and Microwave Assisted Extraction (MAE) of Functional Compounds from Plant Materials. *TrAC Trends Anal. Chem.* **2017**, *97*, 159–178. [[CrossRef](#)]
5. Delazar, A.; Nahar, L.; Hamedeyazdan, S.; Sarker, S.D. Microwave-Assisted Extraction in Natural Products Isolation. *Nat. Prod. Isol.* **2012**, *864*, 89–115.
6. Park, S.-Y.; Karthivashan, G.; Ko, H.M.; Cho, D.-Y.; Kim, J.; Cho, D.J.; Ganesan, P.; Su-Kim, I.; Choi, D.-K. Aqueous Extract of *Dendropanax moribiferus* Leaves Effectively Alleviated Neuroinflammation and Behavioral Impediments in Mptp-Induced Parkinson's Mouse Model. *Oxidative Med. Cell. Longev.* **2018**, *2018*, 3175214. [[CrossRef](#)]
7. Park, Y.M.; Han, J.S. A Study on the Utilization of *Dendropanax moribifera* Lev. Leaf Extract for Material of Functional Cosmetics and Hair Growth Products. *Asian J. Beauty Cosmetol.* **2006**, *14*, 277–288. [[CrossRef](#)]
8. Kim, J.M.; Park, S.K.; Guo, T.J.; Kang, J.Y.; Ha, J.S.; Lee, D.S.; Lee, U.; Heo, H.J. Anti-Amnesic Effect of *Dendropanax moribifera* via Jnk Signaling Pathway on Cognitive Dysfunction in High-Fat Diet-Induced Diabetic Mice. *Behav. Brain Res.* **2016**, *312*, 39–54. [[CrossRef](#)]
9. Kim, W.; Kim, D.W.; Yoo, D.Y.; Jung, H.Y.; Nam, S.M.; Kim, J.W.; Hong, S.-M.; Kim, D.-W.; Choi, J.H.; Moon, S.M.; et al. *Dendropanax moribifera* Léveille Extract Facilitates Cadmium Excretion and Prevents Oxidative Damage in the Hippocampus by Increasing Antioxidant Levels in Cadmium-Exposed Rats. *BMC Complement. Altern. Med.* **2014**, *14*, 428. [[CrossRef](#)]
10. Balakrishnan, R.; Cho, D.Y.; Su-Kim, I.; Choi, D.K. *Dendropanax moribifera* and Other Species from the Genus *Dendropanax*: Therapeutic Potential of Its Traditional Uses, Phytochemistry, and Pharmacology. *Antioxidants* **2020**, *9*, 962. [[CrossRef](#)]
11. Kim, J.Y.; Yoon, J.-Y.; Sugiura, Y.; Lee, S.-K.; Park, J.-D.; Song, G.-J.; Yang, H.-J. *Dendropanax moribiferus* Leaf Extract Facilitates Oligodendrocyte Development. *R. Soc. Open Sci.* **2019**, *6*, 190266. [[CrossRef](#)] [[PubMed](#)]
12. Yang, H.Y.; Kim, K.S.; Lee, Y.H.; Park, J.H.; Kim, J.-H.; Lee, S.-Y.; Kim, Y.-M.; Kim, I.S.; Kacew, S.; Lee, B.M.; et al. *Dendropanax moribifera* Ameliorates Thioacetamide-Induced Hepatic Fibrosis Via Tgf-B1/Smads Pathways. *Int. J. Biol. Sci.* **2019**, *15*, 800–811. [[CrossRef](#)] [[PubMed](#)]
13. Choi, J.; Kim, S. Antioxidant and Antithrombotic Properties of *Dendropanax moribifera* Léveille (Araliaceae) and Its Ferments Produced by Fermentation Processing. *J. Food Biochem.* **2019**, *43*, e13056. [[CrossRef](#)]
14. Youn, J.S.; Kim, Y.-J.; Na, H.J.; Jung, H.R.; Song, C.K.; Kang, S.Y.; Kim, J.Y. Antioxidant Activity and Contents of Leaf Extracts Obtained from *Dendropanax moribifera* Lev Are Dependent on the Collecting Season and Extraction Conditions. *Food Sci. Biotechnol.* **2019**, *28*, 201–207. [[CrossRef](#)] [[PubMed](#)]
15. Akram, M.; Kim, K.A.; Kim, E.S.; Syed, A.S.; Kim, C.Y.; Lee, J.S.; Bae, O.N. Potent Anti-Inflammatory and Analgesic Actions of the Chloroform Extract of *Dendropanax moribifera* Mediated by the Nrf2/Ho-1 Pathway. *Biol. Pharm. Bull.* **2016**, *39*, 728–736. [[CrossRef](#)]
16. Birhanu, B.T.; Kim, J.-Y.; Hossain, A.; Choi, J.-W.; Lee, S.-P.; Park, S.-C. An in Vivo Immunomodulatory and Anti-Inflammatory Study of Fermented *Dendropanax moribifera* Léveille Leaf Extract. *BMC Complement. Altern. Med.* **2018**, *18*, 222. [[CrossRef](#)] [[PubMed](#)]
17. Yoo, D.-Y.; Jung, H.Y.; Kwon, H.J.; Kim, J.W.; Nam, S.M.; Chung, J.Y.; Choi, J.H.; Kim, D.W.; Yoon, Y.S.; Hwang, I.K. Effects of *Dendropanax moribifera* Léveille Extract on Hypothyroidism-Induced Oxidative Stress in the Rat Hippocampus. *Food Sci. Biotechnol.* **2016**, *25*, 1761–1766. [[CrossRef](#)]
18. Lee, J.W.; Kim, K.S.; An, H.K.; Kim, C.H.; Moon, H.I.; Lee, Y.C. Dendropanoxide Induces Autophagy through Erk1/2 Activation in Mg-63 Human Osteosarcoma Cells and Autophagy Inhibition Enhances Dendropanoxide-Induced Apoptosis. *PLoS ONE* **2013**, *8*, e83611. [[CrossRef](#)]
19. Sachan, R.; Kundu, A.; Dey, P.; Son, J.Y.; Kim, K.S.; Lee, D.E.; Kim, H.R.; Park, J.H.; Lee, S.H.; Kim, J.-H.; et al. *Dendropanax moribifera* Protects against Renal Fibrosis in Streptozotocin-Induced Diabetic Rats. *Antioxidants* **2020**, *9*, 84. [[CrossRef](#)]
20. An, N.Y.; Kim, J.E.; Hwang, D.; Ryu, H.K. Anti-Diabetic Effects of Aqueous and Ethanol Extract of *Dendropanax moribifera* Leveille in Streptozotocin-Induced Diabetes Model. *J. Nutr. Health* **2014**, *47*, 394–402. [[CrossRef](#)]
21. Lee, C.; Yang, M.; Moon, J.-O. Antioxidant and Hepatoprotective Effects of the Ethanol Extract of *Dendropanax moribifera* Leveille on the T-Butyl Hydroperoxide-Induced Hepg2 Cell Damages. *Korean J. Pharmacogn.* **2019**, *50*, 32–36.
22. Bae, D.; Kim, J.; Lee, S.-Y.; Choi, E.-J.; Jung, M.-A.; Jeong, C.S.; Na, J.-R.; Kim, J.-J.; Kim, S. Hepatoprotective Effects of Aqueous Extracts from Leaves of *Dendropanax moribifera* Leveille against Alcohol-Induced Hepatotoxicity in Rats and In Vitro Anti-Oxidant Effects. *Food Sci. Biotechnol.* **2015**, *24*, 1495–1503. [[CrossRef](#)]
23. Song, J.H.; Kwak, S.; Kim, H.; Jun, W.; Lee, J.; Yoon, H.G.; Choi, K.C. *Dendropanax moribifera* Branch Water Extract Increases the Immunostimulatory Activity of Raw264. 7 Macrophages and Primary Mouse Splenocytes. *J. Med. Food* **2019**, *22*, 1136–1145. [[CrossRef](#)] [[PubMed](#)]

24. Kim, R.-W.; Lee, S.-Y.; Kim, S.-G.; Heo, Y.-R.; Son, M.-K. Antimicrobial, Antioxidant and Cytotoxic Activities of *Dendropanax morbifera* Léveillé Extract for Mouthwash and Denture Cleaning Solution. *J. Adv. Prosthodont.* **2016**, *8*, 172–180. [[CrossRef](#)] [[PubMed](#)]
25. Chung, I.-M.; Kim, M.-Y.; Park, S.-D.; Park, W.-H.; Moon, H.-I. In Vitro Evaluation of the Antiplasmodial Activity of *Dendropanax morbifera* against Chloroquine-Sensitive Strains of Plasmodium Falciparum. *Phytother. Res.* **2009**, *23*, 1634–1637. [[CrossRef](#)]
26. Yun, J.-W.; Kim, S.-H.; Kim, Y.-S.; Choi, E.J.; You, J.-R.; Cho, E.-Y.; Yoon, J.-H.; Kwon, E.; Kim, H.-C.; Jang, J.-J.; et al. Preclinical Study of Safety of *Dendropanax morbifera* Leveille Leaf Extract: General and Genetic Toxicology. *J. Ethnopharmacol.* **2019**, *238*, 111874. [[CrossRef](#)]
27. Chung, I.-M.; Seo, S.-H.; Kang, E.-Y.; Park, S.-D.; Park, W.-H.; Moon, H.-I. Chemical Composition and Larvicidal Effects of Essential Oil of *Dendropanax morbifera* against *Aedes aegypti* L. *Biochem. Syst. Ecol.* **2009**, *37*, 470–473. [[CrossRef](#)]
28. Lee, S.Y.; Choi, E.J.; Bae, D.H.; Lee, D.W.; Kim, S. Effects of 1-Tetradecanol and B-Sitosterol Isolated from *Dendropanax morbifera* Lev. On Skin Whitening, Moisturizing and Preventing Hair Loss. *J. Soc. Cosmet. Sci. Korea* **2015**, *41*, 73–83. [[CrossRef](#)]
29. Shin, D.C.; Kim, G.C.; Song, S.Y.; Kim, H.J.; Yang, J.C.; Kim, B. Antioxidant and Antiaging Activities of Complex Supercritical Fluid Extracts from *Dendropanax morbifera*, *Corni fructus* and *Lycii fructus*. *Korea J. Herbol.* **2013**, *28*, 95–100. [[CrossRef](#)]
30. Alvand, Z.M.; Rajabi, H.R.; Mirzaei, A.; Masoumiasl, A. Ultrasonic and Microwave Assisted Extraction as Rapid and Efficient Techniques for Plant Mediated Synthesis of Quantum Dots: Green Synthesis, Characterization of Zinc Telluride and Comparison Study of Some Biological Activities. *New J. Chem.* **2019**, *43*, 15126–15138. [[CrossRef](#)]
31. Moon, J.-Y.; Ngoc, L.T.N.; Chae, M.; Van Tran, V.; Lee, Y.-C. Effects of Microwave-Assisted *Opuntia humifusa* Extract in Inhibiting the Impacts of Particulate Matter on Human Keratinocyte Skin Cell. *Antioxidants* **2020**, *9*, 271. [[CrossRef](#)] [[PubMed](#)]
32. Waterman, P.G.; Mole, S. *Analysis of Phenolic Plant Metabolites*; Blackwell Scientific: Hoboken, NJ, USA, 1994.
33. Woisky, R.G.; Salatino, A. Analysis of Propolis: Some Parameters and Procedures for Chemical Quality Control. *J. Apic. Res.* **1998**, *37*, 99–105. [[CrossRef](#)]
34. Mingle, C.E.; Newsome, A.L. An Amended Potassium Persulfate Abts Antioxidant Assay Used for Medicinal Plant Extracts Revealed Variable Antioxidant Capacity Based Upon Plant Extraction Process. *bioRxiv* **2020**. [[CrossRef](#)]
35. Suganya, P.; Jeyaprakash, K.; Mallavarapu, G.R.; Murugan, R. Comparison of the Chemical Composition, Tyrosinase Inhibitory and Anti-Inflammatory Activities of the Essential Oils of *Pogostemon plectranthoides* from India. *Ind. Crops Prod.* **2015**, *69*, 300–307. [[CrossRef](#)]
36. Tu, P.T.B.; Tawata, S. Anti-Oxidant, Anti-Aging, and Anti-Melanogenic Properties of the Essential Oils from Two Varieties of *Alpinia zerumbet*. *Molecules* **2015**, *20*, 16723–16740. [[CrossRef](#)]
37. Park, C.; Kim, J.; Hwang, W.; Lee, B.D.; Lee, K. In Vitro Anti-Tyrosinase Activity of Viscumneoside III and Homoflavoyadorinin B Isolated from Korean Mistletoe (*Viscum album*). *Korean J. Plant Resour.* **2016**, *29*, 690–698. [[CrossRef](#)]
38. Casagrande, R.; Georgetti, S.R.; Verri, W.; Dorta, D.; Santos, A.C.; Fonseca, M.J. Protective Effect of Topical Formulations Containing Quercetin against Uvb-Induced Oxidative Stress in Hairless Mice. *J. Photochem. Photobiol. B Biol.* **2006**, *84*, 21–27. [[CrossRef](#)]
39. Fulop, T.; Khalil, A.; Larbi, A. The Role of Elastin Peptides in Modulating the Immune Response in Aging and Age-Related Diseases. *Pathol. Biol.* **2012**, *60*, 28–33. [[CrossRef](#)]
40. Thring, T.S.; Hili, P.; Naughton, D.P. Anti-Collagenase, Anti-Elastase and Anti-Oxidant Activities of Extracts from 21 Plants. *BMC Complement. Altern. Med.* **2009**, *9*, 27. [[CrossRef](#)]
41. Horng, C.-T.; Wu, H.-C.; Chiang, N.-N.; Lee, C.-F.; Huang, Y.-S.; Wang, H.-Y.; Yang, J.-S.; Chen, F.-A. Inhibitory Effect of Burdock Leaves on Elastase and Tyrosinase Activity. *Exp. Ther. Med.* **2017**, *14*, 3247–3252. [[CrossRef](#)]
42. Popoola, O.K.; Marnewick, J.L.; Rautenbach, F.; Ameer, F.; Iwuoha, E.I.; Hussein, A.A. Inhibition of Oxidative Stress and Skin Aging-Related Enzymes by Prenylated Chalcones and Other Flavonoids from *Helichrysum teretifolium*. *Molecules* **2015**, *20*, 7143–7155. [[CrossRef](#)] [[PubMed](#)]
43. Villareal, M.O.; Kume, S.; Neffati, M.; Isoda, H. Upregulation of Mitf by Phenolic Compounds-Rich *Cymbopogon schoenanthus* Treatment Promotes Melanogenesis in B16 Melanoma Cells and Human Epidermal Melanocytes. *BioMed Res. Int.* **2017**, *2017*, 8303671. [[CrossRef](#)] [[PubMed](#)]
44. Lin, Y.-S.; Chen, H.-J.; Huang, J.-P.; Lee, P.-C.; Tsai, C.-R.; Hsu, T.-F.; Huang, W.-Y. Kinetics of Tyrosinase Inhibitory Activity Using *Vitis vinifera* Leaf Extracts. *BioMed Res. Int.* **2017**, *2017*, 5232680. [[CrossRef](#)]
45. Kim, Y.-J.; Uyama, H.; Kobayashi, S. Inhibition Effects of (+)-Catechin-Aldehyde Polycondensates on Proteinases Causing Proteolytic Degradation of Extracellular Matrix. *Biochem. Biophys. Res. Commun.* **2004**, *320*, 256–261. [[CrossRef](#)] [[PubMed](#)]
46. Baylac, S.; Racine, P. Inhibition of Human Leukocyte Elastase by Natural Fragrant Extracts of Aromatic Plants. *Int. J. Aromather.* **2004**, *14*, 179–182. [[CrossRef](#)]